

# Mechanical and Degradation Properties of Castor Oil-Based Polyurethane

Yasaman Ganji, Mehran Kasra, Soheila Salahshour Kordestani

**Abstract**— Castor oil based polyurethanes (PU) with different degradation and mechanical properties have many applications both in industry and medicine. In this study, polyethylene glycol (PEG), castor oil (CO) and 1, 6 -hexamethylene diisocyanate (HDI) were used for synthesis of different kinds of vegetable oil based polyurethanes. Five different chemical compositions of PU with different molar ratios of PEG, CO, and HDI were prepared and casted as solid and porous samples. The samples were then characterized by Fourier transform infrared spectroscopy, dynamic mechanical thermal analysis, and differential scanning calorimetry. Changes in mechanical properties, degradation rate, density, and contact angle were also studied. The results showed that degradation and mechanical properties were related to the ratio of castor oil to polyethylene glycol which made these properties controllable. These properties were also affected by the porosity, as storage and loss moduli were decreased and degradation rate was increased in porous samples compared to those of solid ones.

**Index Terms**— Biomaterials, Degradation, Polyurethane, viscoelastic properties.

## I. INTRODUCTION

Polyurethanes (PUs) are an interesting class family of elastomers. These synthetic materials consist of repeated blocks of hard and soft segments. The arrangement of these segments provides unique properties and a wide range of application for polyurethanes [1]. Considering mechanical and chemical properties, controllable degradation and biostability, biocompatibility, and hemocompatibility makes PUs an outstanding material in medicine [2, 3]. Poly (ether) urethanes are widely used for long term applications in tissues such as heart, liver, blood vessels, and urinary system due to their biostability [4, 5]. However, poly (ester) urethanes are degradable and used as a matrix for engineered tissues [6, 7].

Using vegetable oils as a polyol in PU synthesis leads to biodegradable polyurethanes with many medical applications such as cardiovascular system regeneration [8], peripheral nerve regeneration [9], cartilage and meniscus engineering [10], trabecular bone replacement [11], and controlled drug delivery systems [12]. Bio-based PUs in comparison with petrochemical derived PUs showed lower crystallinity which led to lower stress concentration, and consequently the improvement of mechanical properties [7].

### Manuscript Received on April 2015.

**Yasaman Ganji**, Faculty of Biomedical Engineering, Amirkabir University of Technology, Tehran, Iran.

**Mehran Kasra**, Faculty of Biomedical Engineering, Amirkabir University of Technology, Tehran, Iran.

**Soheila Salahshour Kordestani**, Faculty of Biomedical Engineering, Amirkabir University of Technology, Tehran, Iran.

The authors gratefully acknowledge the financial support of this research by Iran National Science Foundation (INSF project No. 90008011).

Among all vegetable oils, castor oil (CO) is the most famous source of ricinoleic acid with three functional hydroxyl groups, which can be directly used in PU synthesis as the soft segment or chain extender without any further modification to functionalize it [13]. Castor oil, with a hydroxyl functional group on the 12th carbon [14], has a very low toxicity as well as a low cost making it a valuable renewable agriculture resource [15].

In previous studies, it has been shown that castor oil based PUs are almost stable in a saline buffer for a time period of 95 days. However, adding polyethylene glycol (PEG) increased the degradation rate [13]. Polyethylene glycol as a hydrophilic polyol increases water permeability in bulk as well as surface and make the material more susceptible to degradation with non – toxic degradation products [16]. Hydrolysis is the most common mechanism of in-vivo degradation in this kind of PUs [17]. Therefore, polyurethanes based on castor oil and polyethylene glycol are ideal materials for biomedical implants and tissue engineering applications due to their controllable degradation and wide range of mechanical properties. These kinds of polyurethanes also showed shape memory properties [18].

In urethane synthesis, an active hydrogen atom of hydroxyl group reacts with the NCO group in isocyanate and a urethane band is formed. Therefore, the ratio of NCO to OH plays an important role in final properties. The NCO/OH ratio of one, omits any un-functional isocyanate groups [19]. Santos et al. [1] showed that additional NCOs could change the chemical properties of PU, even if they reacted completely with air humidity or water content of polyol. Additional polyol weakened the polymer mechanically due to large distances among urethane groups and low cross linking [1].

There are many different methods in scaffold fabrication. Electro-spinning and 3D printing are used for thin layer of tissue while porogen leaching and solvent casting methods provide a thick scaffold making the pore size and the percentage of porosity controllable. High interconnectivity of pores is a challenge in porogen leaching method [20] which can be enhanced by selecting the size and amount of the added salt particles.

In the present work, we aimed to synthesize and characterize different kinds of polyurethanes based on castor oil and polyethylene glycol. Different molar ratios of castor oil, polyethylene glycol, and hexa-methylene diisocyanate (HDI) were prepared and casted in the forms of solid and porous scaffolds. The effects of the chemical composition of materials on the surface, thermal, and viscoelastic properties were examined by contact angle measurements, differential scanning calorimetry (DSC), and dynamic mechanical thermal analysis (DMTA). By comparing the mechanical properties and degradation rate of the solid and porous samples, the effect of porosity on these properties was

investigated. To our knowledge, there has been no study comparing the properties of porous castor oil based polyurethane samples with those of solid ones. Testing different polyurethanes composites with tunable thermomechanical properties and degradation rates, this study provides new data on the properties of porous renewable resources-based polyurethanes.

## II. MATERIALS AND METHODS

### A. Materials

Castor oil (Sigma-Aldrich, Germany), Polyethylene glycol 2000 (Merck, Germany), 1, 6-Hexa-methylene diisocyanate (HDI, Merck, Germany), were used for polyurethane synthesis. All the materials were used as received without any further modification. Lysozyme (Sigma-Aldrich, Germany) was used for degradation study.

### B. Polyurethane Synthesis

HDI, 20 wt. % aqueous solutions of PEG, and castor oil (with hydroxyl number of 2.7) with different molar ratios (PPUs) were mechanically mixed for 150 min at 70 °C under N<sub>2</sub> atmosphere. The mixture was casted in a Teflon mold and dried at room temperature for 2 days. Another solution of HDI and castor oil with the molar ratio of 3:2 (MPU) was mechanically mixed for 120 min at 70 °C under N<sub>2</sub> atmosphere. A 30 wt. % solution of PPUs in chloroform was added to MPU and mixed for an extra 30 min to obtain a homogenous solution. Final chemical compositions of all the samples were presented in Table 1. Five groups of the PU samples (PU1 to PU5) were made by changing the ratio of CO:PEG:HDI from 4:0:4 in PU1 to 0:4:4 in PU5 (Table 1). The amounts of HDI, PEG and CO were adjusted in a way that a 1:1 molar ratio of hydroxyl and NCO groups was established to omit any un-reacted NCO.

A part of the solution was casted in a Teflon mold having a 10 mm diameter and 4 mm thickness for preparing of the solid discs. Another part of solution was casted in a strip-shape Teflon mold with the dimension of 80×6×4 mm for preparing of the tensile testing samples. For fabrication of the porous discs, 106-355 μm sieved table salt was added to the remaining solution and then centrifuged at 2000 rpm for 10 min [20]. The extra solution was removed, and the mixture of polymer and salt was casted in the Teflon mold with the same dimension of the solid strips and solid discs. Afterwards, all the samples were dried at room temperature for 48 h, and the porous samples were placed in water for 2 more days to

**Table 1 Chemical composition of the PU samples.**

code	HDI (gr)	CO (gr)	PEG (gr)	Molar ratio of CO:PEG:HDI
PU1	15.29	56.48	-	4:0:4
PU2	18.68	51.77	1.13	3:1:4
PU3	23.36	43.1	2.83	2:2:4
PU4	33.64	31.06	6.12	1:3:4
PU5	56.06	-	13.60	0:4:4

remove the salt. The samples floated in water when the salt has completely removed.

### C. Characterization

For morphological analyses, the samples were coated with a thin layer of gold by sputtering machine (Ion Tech Ltd.,

Teddington, U.K.), and then a scanning electron microscope (SEM) (Philips XL 20, Philips Export B.V. Eindhoven, The Netherlands) was used to image the samples.

In the water uptake and degradation studies, 3 porous and 3 solid discs of each chemical composition were placed in 10 ml of water and kept for up to 28 days in a humidified incubator at 37°C. The samples were removed from water after 3, 7, 14 and 28 days and weighed with an analytical balance. The percentage of water uptake was calculated according to the following equation:

$$\text{Water uptake (\%)} = (m_{\text{wet}} - m_0)/m_0 \times 100, \quad (1)$$

where  $m_0$  and  $m_{\text{wet}}$  were the dry and wet masses of samples, respectively.

A 0.1 wt. % solution of lysozyme in DMEM culture medium was prepared as an enzymatic degradation solution. Dried porous and solid discs were weighed with the accuracy of 0.1 mg ( $m_0$ ) and placed into 10 ml of degradation solution. All the samples were incubated at 37°C for 28 days. For each chemical series, 3 samples were removed after 3, 7, 14, and 28 days, washed with distilled water and dried at room temperature for 72 h. Then the samples were weighed ( $m_d$ ) and percentage of weight loss was determined based on the following equation:

$$\text{Weight loss (\%)} = (m_0 - m_d)/m_0 \times 100. \quad (2)$$

Apparent densities of the porous and solid discs were calculated by dividing the dried weight ( $m_d$ ) by the specimen volume based on dimensions of their cylindrical geometry.

KRUSS-K14 digital surface tension measuring system (Kruss, Germany) was used to determine polar and disperse surface energies as well as contact angle according to Owens-Wendt-Rabel-Kaeble method [21]. The measurements were performed at room temperature with two different liquids of water and formamide.

A BOMEM Fourier transform infrared (FTIR) spectrophotometer was used to observe the chemical composition of the samples within the wave numbers of 600 to 4000 cm<sup>-1</sup>.

Changes in the mechanical properties, tensile and compressive moduli, were investigated by performing compression and tensile tests. For the compression study, porous and solid discs with the diameter of 10 mm and the thickness of 4 mm were placed in a DTM (Dynamic Test Machine, Zwick/Roller, UTM HTC 400/25, Germany) and exposed to a deformation rate of 0.5 mm/min. Tension tests were applied on the porous and solid strips with the dimension of 80×6×4 mm with a deformation rate of 10 mm/min. Each measurement was repeated with 3 different samples.

Dynamic mechanical thermal analysis (DMTA) of samples were performed in a Triton DMTA machine (TTDMA model, UK), at 3 different frequencies of 0.1, 1 and 10 Hz at room temperature in a compression mode using solid and porous discs. The displacement loading amplitude was set at 20 μm.

Enthalpy changes of samples indicating glass temperature (T<sub>g</sub>), crystallinity temperature (T<sub>c</sub>), and heat of fusion (ΔH<sub>f</sub>) were examined using a Mettler Toledo differential scanning calorimetry (DSC) machine in a temperature range of -50 to 200 °C at a heating rate of 10 °C/min.

### D. Statistical Analysis

Analysis of variance (ANOVA) followed by Tukey's multiple comparison test were used to determine significant differences in mechanical properties with a  $p < 0.05$ .

### III. RESULTS AND DISCUSSION

SEM images of porous samples are shown in Fig.1. High interconnectivity of pores was enhanced by combining the centrifugation of salt with the salt leaching method suggested by Sin et al. [20]. The pores showed a quite uniform size and distribution with the average size of ~300  $\mu\text{m}$ .

Figs 2 and 3 show the water uptake and degradation of samples in a time period of 28 days, respectively. Water uptake for solid discs showed a non linear trend in a 28-day period of time (Fig. 2a), whereas this trend for all porous discs was completely linear (Fig. 2b). In solid discs water uptake decreased after 14 days. For both solid and porous samples, the lowest values of water uptake were related to PU1 without any polyethylene glycol in all time points. In general, water uptake was in the range of 5 to % 80 for solid discs and 100 to % 250 for porous discs.

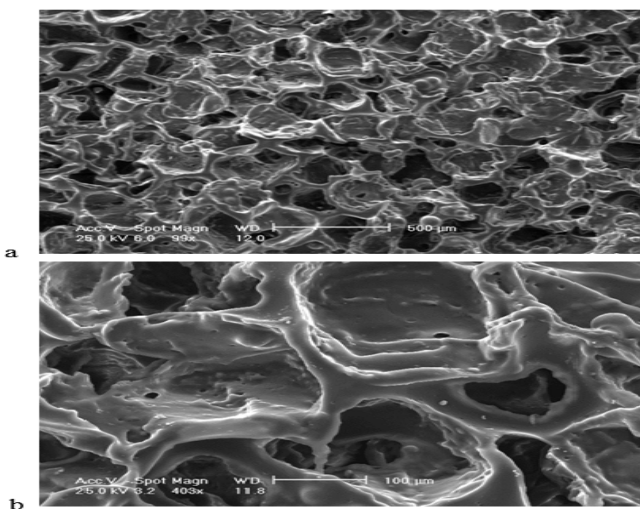


Fig. 1 SEM images of porous samples of interconnected pores shown in (a) small and (b) large magnifications.

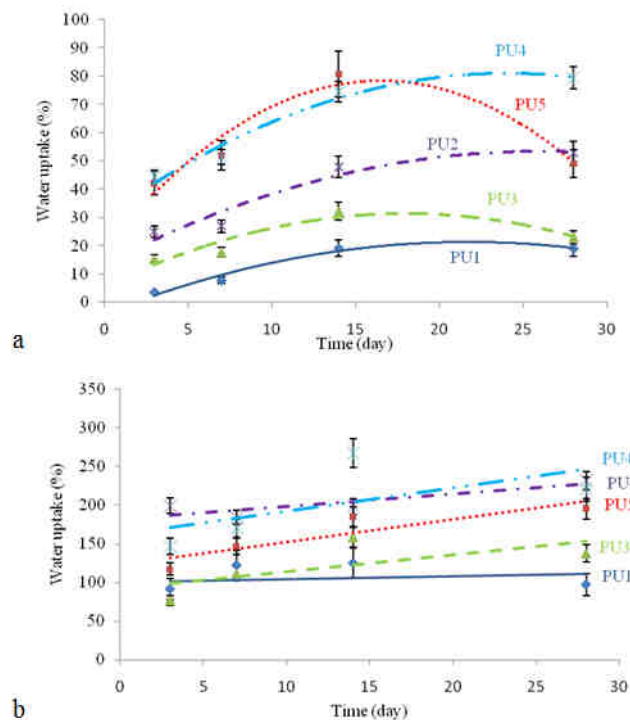


Fig. 2 Water uptake of (a) solid and (b) porous discs in a time period of 4 weeks.

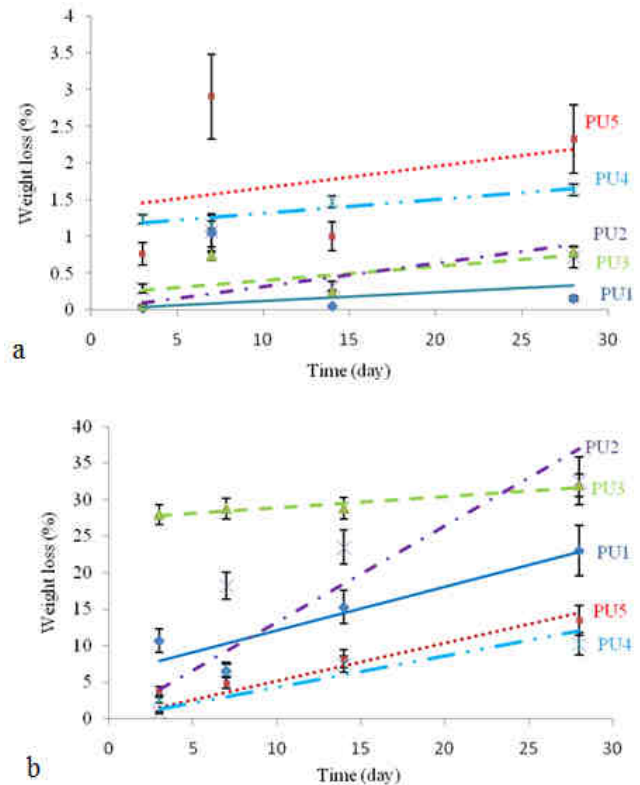


Fig. 3 Degradation of (a) solid and (b) porous discs in a time period of 4 weeks.

Enzymatic degradations of PU discs were also investigated for both solid and porous discs using a 0.1 wt. % solution of lysozyme in DMEM culture medium (Fig. 3). The ratios of degradation rates for porous scaffolds to those of solid ones were calculated to be; 49, 42, 8, 23 and 18 for PU1, PU2, PU3, PU4 and PU5, respectively. Therefore, porosity was obviously helpful in bulk degradation. The weight loss was higher for PU5 (containing the most amount of PEG) in solid discs compared to those of other solid PUs in all time points. However, the degradation rate of porous discs had the highest value of % 1.32 per day for PU2.

The values of density for both solid and porous discs were provided in Table 2. The highest and lowest values of density in both solid and porous discs were related to PU1 and PU4, respectively.

Contact angle values as well as surface tension energies were also presented in Table 2. Water and formamide were used to measure surface tension and contact angle values. The surface energy of a material can be described as being the sum of the polar and disperse interaction parts. The bonding of an adjacent material depends on how similar the two materials are with respect to the polar and disperse part of energy. PU5 and PU2 showed the lowest (81.9) and highest (88.5) values of water contact angles respectively (Table 2).

The presence of urethane band was confirmed as shown in Fig. 4. Amine stretching band and hydrogen bonded N-H vibration band were stronger in those samples of PU3, PU4 and PU5 at about 3340  $\text{cm}^{-1}$ . O-H stretching of carboxylic acid group showed a strong yoke shape peak at about 2850 and 2930  $\text{cm}^{-1}$  in those samples of PU1 and PU3. Urethane band for PU1 as the control sample was observed at 1745  $\text{cm}^{-1}$  which was related to the stretching vibration modes of



ester group. Another peak in this sample was amide C=O stretching at 1649 cm<sup>-1</sup>. This peak was also appeared in PU5 and PU3 at about 1620 cm<sup>-1</sup>. C–N stretching vibration modes were observed in PU3 at 1274 and 1241 cm<sup>-1</sup>, PU4 at 1278 and 1235 cm<sup>-1</sup>, and PU5 at 1278 and 1240 cm<sup>-1</sup>. Ether stretching vibration was only observed in PU3 and PU5 at 1145 and 1161 cm<sup>-1</sup>, respectively.

Compressive and tensile moduli for solid PU discs are shown in Fig. 5. PU5 with the highest amount of PEG had the highest values for both compressive and tensile moduli. The compressive modulus of PU1 without any PEG and the tensile modulus of PU2 had the least values of the compressive and tensile moduli respectively. All the values in each data series were significantly different (*p* < 0.05) except that of compressive modulus between PU3 and PU4 (as indicated with star symbols in Fig. 5). Similarly, the compressive and tensile moduli for the porous PU discs are presented in Fig. 6. There were no significant differences between compressive moduli of porous PU1 and PU4. All the other values in both data series of compressive and tensile moduli were significantly different (*p* < 0.05). The lowest value of compressive modulus was related to porous PU2. In tensile tests, porous PU1 without any PEG showed the highest value of modulus with a large difference compared to the other porous PUs.

The influence of higher amount of PEG also translated to higher amount of crystalline domains in the polymer. These crystalline domains changed the viscoelastic and thermal properties of the samples in other studies [13]. Viscoelastic properties of the solid discs were represented by tan δ, storage modulus (E') and loss modulus (E'') (Table 3). In all of the solid discs, tan δ increased by increasing the frequency with the highest values belonging to those of PU2 samples. For storage modulus, the trends were almost constant for different chemical compositions except those of PU2 and PU3 in which a slight increase of storage modulus was shown at higher

frequencies. Loss modulus also showed an increasing trend in all samples with frequency. PU3 had the highest value of loss modulus at all frequencies.

The viscoelastic properties of the porous discs were presented in Table 4. All the properties, tan δ, storage modulus (E'), and loss modulus (E'') showed exactly the same trend of those of the solid discs. Comparing the data of the solid discs properties (Table 3) with those of the porous ones (Table 4) indicated that porosity caused an increase of about % 57 in tan δ and decreases of % 33 and % 51 in storage (E') and loss (E'') moduli respectively.

DSC curves for different PU composites are shown in Fig. 7. In this figure, no exothermic or endothermic peak was observed in PU1 without PEG. Biological polyols lead to presence of some crystalline domains in polymeric matrix [22] which was observed in other samples except PU1. Glass transition temperature for PU1 was – 30.35 °C, and this low temperature confirmed the elasticity and softness of material [9]. At glass temperatures above zero, the elasticity would be limited by hard segments of material leading to higher mechanical properties [9, 22]. The exothermic peaks at 27.4, 56.8, 58.9 and 55.8 °C for PU2, PU3, PU4 and PU5 respectively (Fig. 7) were related to the degree of crystallinity caused by PEG.

Castor oil is a naturally occurring vegetable oil consists of 90% ricinoleic acid and 10% oleic and linoleic acids. The functionality of CO is caused by hydroxyl group and is 2.7. The functionality of PEG2000 is also 1.96. In urethane synthesis, an active hydrogen atom of hydroxyl group reacts with the NCO group in isocyanate and a urethane band is formed. HDI has 2 NCO groups. Therefore, for a complete urethane synthesis, the NCO/OH ratio of one should be considered in calculations [23].

**Table 2 Density, contact angle, and surface tension of different PU compositions.**

parameter		PU1	PU2	PU3	PU4	PU5
Density (g/cm <sup>3</sup> )	solid	0.721	0.914	0.893	0.629	0.73
	porous	0.367	0.531	0.504	0.346	0.425
Contact angle (water)		82.7	88.5	86.8	82.2	81.9
Contact angle (formamide)		70.8	87.6	88	74.8	74.6
Surface tension (mN/m)		26.1	19.2	20.6	24.3	24.5
Disperse part (mN/m)		16.6	5	3.9	11.8	11.7
Polar part (mN/m)		9.5	14.2	16.7	12.6	12.8

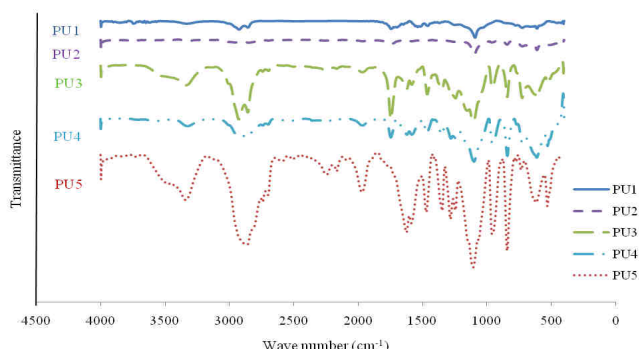


**Fig. 4 FTIR spectra of polyurethane samples.**

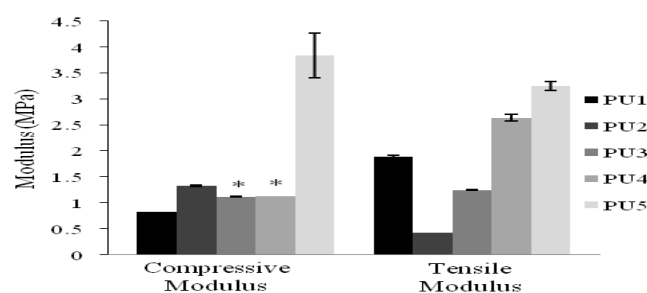


**Fig. 5 Compressive and tensile moduli for the solid PU discs. All the values are significantly different except those indicated by the symbol "\*" (*p* < 0.05).**

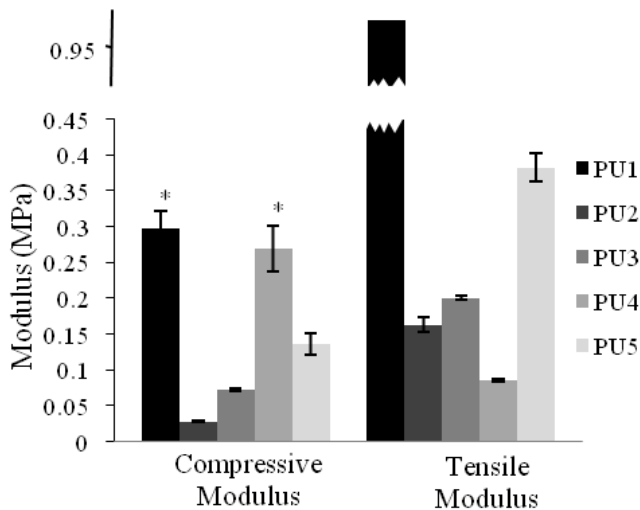


**Fig. 6 Compressive and tensile moduli for the porous PU discs. All the values are significantly different except those indicated by the symbol "\*" ( $p < 0.05$ ).**

In the present study, CO, PEG and HDI were used to synthesis different composition of polyurethane with solid and porous structure, and the role of porosity in mechanical and structural properties was investigated. Salt leaching method was used to fabricate the porous structures. The average pore size in the range of 200-500  $\mu\text{m}$  has been

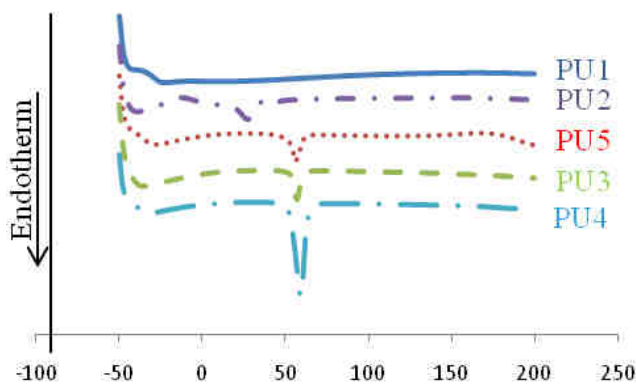


**Fig. 7 DSC thermograph of different PU composition.**

considered as the proper size for tissue engineering applications [20]. In our experiments, using meshed salts in the range of 106-355  $\mu\text{m}$  resulted in an average pore size of 300  $\mu\text{m}$  (Fig. 1). These porous structures affected the water

uptakes and degradation rates of samples (Fig. 2 and 3). Water uptakes in porous discs were 4 to 5 times higher than those of solid discs. Degradation rates were also higher in porous discs compared to those of solid discs. It has been suggested that PEG improved hydrolytic degradation and compared to other vegetable oils, castor oil changed water permeability and degradation from bulk [22]. In our experiment, both the enzymatic and hydrolytic degradation played a role in weight loss. Comparing the weight loss in solid discs (up to % 2.5) with those of porous discs (up to % 35) indicated the role of porosity in accelerating the degradation process (Fig. 3).

Surface properties and contact angle play an important role in biomedical applications regarding to the interaction of cells and tissues with the scaffold material. An optimum value of contact angle for fibroblast cell attachment is in the range of 60 - 80° [24, 25]. In our experiment, the values of water contact angles varied from 81.9 to 88.5. Polar part of energy, as an important driving force for cell attachment in medical applications, also varied from 9.5 mN m<sup>-1</sup> for PU1 to 16.7 mN m<sup>-1</sup> for PU3 (Table 2).

Investigation of mechanical properties of samples showed the dependency of the mechanical properties to chemical composition as well as porosity (Figs. 5 and 6). It has been suggested that the tensile strength of elastomers increased as propylene glycol amount decreased [23]. In our study, the tensile moduli of solid discs increased by increasing the amount of PEG (Fig. 5). However, no relationship was observed between the chemical composition and tensile or compressive moduli. These behaviors could be explained based on increase of intermolecular interactions and crosslink efficiency. In PU1, castor oil was used as the polyol for polyurethane synthesis; however, castor oil acted as the chain extender in those samples containing PEG rather than a polyol [23]. Therefore, crosslink density increased by increasing the amount of PEG, resulted in higher tensile modulus. Different ratios of CO to HDI has been reported to lead to a wide range of tensile moduli from 11 to 300 MPa [7]. In our study, considering the chemical composition of the specimens containing PEG, the tensile modulus for different molar ratios of

**Table 3 tan  $\delta$ , storage modulus ( $E'$ ), and loss modulus ( $E''$ ) of the solid discs obtained from DMTA results.**

Frequency (Hz)	tan $\delta$			Storage Modulus ( $E'$ ) (Pa)			Loss Modulus ( $E''$ ) (Pa)		
	0.1	1	10	0.1	1	10	0.1	1	10
PU1	0.007	0.010	0.031	1299000	1303000	1321000	8811.54	13979.6	40944.6
PU2	0.091	0.174	0.298	265396	309903	415400	24082	54005.3	123736
PU3	0.060	0.114	0.235	966346	1051698	1273115	57990	120144	299447
PU4	0.021	0.042	0.099	683311	703051	758065	14672.6	29609.6	74813.3
PU5	0.032	0.043	0.083	1256267	1292314	1372261	39871.6	55704.8	113928

**Table 4**  $\tan \delta$ , storage modulus ( $E'$ ), and loss modulus ( $E''$ ) of the porous discs obtained from DMTA results.

Frequency (Hz)	$\tan \delta$			Storage Modulus ( $E'$ ) (Pa)			Loss Modulus( $E''$ ) (Pa)		
	0.1	1	10	0.1	1	10	0.1	1	10
PU1	0.013	0.024	0.084	398966	402552	416175	5252.9	9740.9	35218.5
PU2	0.098	0.182	0.340	166608	192321	259284	16341	35023	88158.6
PU3	0.087	0.157	0.295	259231	293632	379605	22590	46092	112032
PU4	0.041	0.067	0.143	180978	189714	211916	7449.6	12794	30367
PU5	0.041	0.065	0.134	241447	253122	281123	9946.5	16502	37714.9

CO:PEG:HDI increased from 0.4 (PU2) to 3.2 MPa (PU5) (Fig. 5), indicating the stiffening effect of PEG in PEG-containing samples.

Investigation of dynamic mechanical thermal behavior of elastomers showed that only a small amount of PEG caused an increase in  $\tan \delta$  (PU2 in our study), and higher amount of PEG decreased this parameter. In other studies, increasing the mass ratio of PEG to CO caused a slight shift in  $\tan \delta$ , associated with glass transition temperature, to lower temperature [13]. This study also reported that the amplitude of  $\tan \delta$  became smaller as PEG content increased. This phenomenon is attributed to the decrease in degree of freedom for segmental mobility of the polymer chain as a result of increase in physically effective crosslink density, as it was already observed in mechanical properties.  $\tan \delta$ , storage modulus ( $E'$ ), and loss modulus ( $E''$ ) showed similar trends in solid and porous discs but in different values (Tables 3 and 4).

Similarly, this phenomena was also observed in DSC results, when the PU1 without any PEG showed no exothermic or endothermic peaks (Fig. 7), and the presence of PEG caused the formation of crystalline domains [22]. This could be translated to typical two-phase behavior related to the PEG–CO segments.

**IV. CONCLUSION**

Porous and solid samples of different compositions of polyurethane using vegetable oil based raw material (castor oil) and polyethylene glycol were prepared and their chemical, mechanical, and degradation properties were studied. Both the compressive and tensile moduli of the solid PUs had the highest values when containing the most amount of PEG (PU4 and PU5). Whereas, in porous samples, the compressive and tensile moduli were higher for those samples without any PEG (PU1). Degradation rate and water uptake were related to both the porosity and chemical composition. Porosity increased the degradation rate of the PUs up to % 49 in a time period of 28 days. PEG also increased the water uptake and weight loss. Controllability of hydrophilicity and degradation rate of this class of PU materials make them very suitable for biomedical applications.

**REFERENCES**

[1] dos Santos D, Tavares L, Batalha G. Mechanical and physical properties investigation of polyurethane material obtained from renewable natural source. *Journal of Achievements in Materials and Manufacturing Engineering* 2012;54:211-7.  
 [2] Chou CW, Hsu S, Wang PH. Biostability and biocompatibility of poly (ether) urethane containing gold or silver nanoparticles in a porcine model. *Journal of Biomedical Materials Research Part A* 2008;84:785-94.

[3] Madbouly SA, Otaigbe JU. Recent advances in synthesis, characterization and rheological properties of polyurethanes and POSS/polyurethane nanocomposites dispersions and films. *Progress in Polymer Science* 2009;34:1283-332.  
 [4] Uttayarat P, Perets A, Li M, Pimton P, Stachelek SJ, Alferiev I, et al. Micropatterning of three-dimensional electrospun polyurethane vascular grafts. *Acta Biomaterialia* 2010;6:4229-37.  
 [5] Jovanovic D, Roukes FV, Löber A, Engels GE, Oeveren W, Seijen XJ, et al. Polyacrylurethanes as Novel Degradable Cell Carrier Materials for Tissue Engineering. *Materials* 2011;4:1705-27.  
 [6] Xu D, Wu K, Zhang Q, Hu H, Xi K, Chen Q, et al. Synthesis and biocompatibility of anionic polyurethane nanoparticles coated with adsorbed chitosan. *Polymer* 2010;51:1926-33.  
 [7] Corcuera M, Rueda L, Fernandez d’Arlas B, Arbelaz A, Marieta C, Mondragon I, et al. Microstructure and properties of polyurethanes derived from castor oil. *Polymer degradation and stability* 2010;95:2175-84.  
 [8] Cauch-Rodríguez JV, Chan-Chan LH, Hernandez-Sánchez F, Cervantes-Uc JM. Degradation of Polyurethanes for Cardiovascular Applications. *Advances in Biomaterials Science and Biomedical Applications: InTech*; 2013. p. 51-82.  
 [9] Li G, Li D, Niu Y, He T, Chen KC, Xu K. Alternating block polyurethanes based on PCL and PEG as potential nerve regeneration materials. *Journal of Biomedical Materials Research Part A* 2013.  
 [10] Werkmeister J, Adhikari R, White J, Tebb T, Le T, Taing H, et al. Biodegradable and injectable cure-on-demand polyurethane scaffolds for regeneration of articular cartilage. *Acta Biomaterialia* 2010;6:3471-81.  
 [11] Nacer RS, Poppi RR, Carvalho PTC, Silva BAK, Odashiro AN, Silva IS, et al. Castor oil polyurethane containing silica nanoparticles as filling material of bone defect in rats. *Acta Cirurgica Brasileira* 2012;27:56-62.  
 [12] Coneski PN, Schoenfisch MH. Synthesis of nitric oxide-releasing polyurethanes with S-nitrosothiol-containing hard and soft segments. *Polymer chemistry* 2011;2:906-13.  
 [13] Yeganeh H, Hojati-Talemi P. Preparation and properties of novel biodegradable polyurethane networks based on castor oil and poly (ethylene glycol). *Polymer degradation and stability* 2007;92:480-9.  
 [14] Ayo M, Madufor I, Ekebafé L, Chukwu M, Tenebe O, Eguare K. Performance Analysis of Castor Oil Based Polyurethane Foam. *International Journal of Basic and Applied Sciences* 2012;1:255-7.  
 [15] Najafabadi SAA, Keshvari H, Ganji Y, Tahriri M, Ashuri M. Chitosan/heparin surface modified polyacrylic acid grafted polyurethane film by two step plasma treatment. *Surface Engineering* 2012.  
 [16] Yeganeh H, Lakouraj MM, Jamshidi S. Synthesis and properties of biodegradable elastomeric epoxy modified polyurethanes based on poly ( $\epsilon$ -caprolactone) and poly (ethylene glycol). *European Polymer Journal* 2005;41:2370-9.  
 [17] Da Silva GR. Biodegradation of polyurethanes and nanocomposites to non-cytotoxic degradation products. *Polymer degradation and stability* 2010;95:491-9.  
 [18] Rio ED, Lligadas G, Ronda J, Galia M, Meier M, Cádiz V. Polyurethanes from polyols obtained by ADMET polymerization of a castor oil-based diene: Characterization and shape memory properties. *Journal of Polymer Science Part A: Polymer Chemistry* 2011;49:518-25.  
 [19] Silva SS, Menezes SMC, Garcia RB. Synthesis and characterization of polyurethane-g-chitosan. *European Polymer Journal* 2003;39:1515-9.  
 [20] Sin DC, Miao X, Liu G, Wei F, Chadwick G, Yan C, et al. Polyurethane (PU) scaffolds prepared by solvent casting/particulate leaching (SCPL) combined with centrifugation. *Materials Science and Engineering: C* 2010;30:78-85.  
 [21] Okuji S, Boldryeva H, Takeda Y, Kishimoto N. Characteristics of poly (vinylidene difluoride) modified by plasma-based ion



implantation. Nuclear Instruments and Methods in Physics Research Section B: Beam Interactions with Materials and Atoms 2009;267:1557-60.

- [22] Kong X, Liu G, Curtis JM. Novel Polyurethane Produced from Canola Oil Based Poly (ether ester) Polyols: Synthesis, Characterization and Properties. European Polymer Journal 2012;48:2097–106.
- [23] Yeganeh H, Mehdizadeh MR. Synthesis and properties of isocyanate curable millable polyurethane elastomers based on castor oil as a renewable resource polyol. European Polymer Journal 2004;40:1233-8.
- [24] Tamada Y, Ikada Y. Effect of preadsorbed proteins on cell adhesion to polymer surfaces. Journal of Colloid and Interface Science 1993;155:334-9.
- [25] Wei J, Igarashi T, Okumori N, Igarashi T, Maetani T, Liu B, et al. Influence of surface wettability on competitive protein adsorption and initial attachment of osteoblasts. Biomedical Materials 2009;4:045002.

**Yasaman Ganji**, Ph.D. student, Faculty of Biomedical Engineering, Amirkabir University of Technology, Tehran, Iran; M.Sc., Tissue Engineering, Faculty of Biomedical Engineering, Amirkabir University of Technology, Tehran, Iran; B.Sc., Materials Science and Engineering, Department of Materials Science and Engineering, Sharif University of Technology, Tehran, Iran; Research fellow, Technical Faculty, Christian-Albrechts-Universität zu Kiel, Kiel, Germany. Research area: Biomaterials, cardiac tissue engineering, composites, polymer synthesis.

**Mehran Kasra**, Associate Professor, Faculty of Biomedical Engineering, Amirkabir University of Technology, Tehran, Iran. Formerly, Associate Professor, Department of Mechanical Engineering, McMaster University, Hamilton, ON, Canada; Associate Professor, Biomedical Engineering, University of Tennessee, Knoxville, TN, USA; Assistant Professor, Biomedical Engineering, University of Iowa, Iowa City, IA, USA. Expertise: Biomechanics, Biomaterials, Tissue Engineering. Degrees: Ph.D., Mechanical Engineering, Ecole Polytechnique de Montreal, Montreal, Canada; M.Eng. Mechanical Engineering, McGill University, Montreal, Canada.

**Soheila Salahshour Kordestani**, Head of Biomaterial Department, Faculty of Biomedical Engineering, Amirkabir University of Technology, Tehran, Iran. Professional experience: Post doctoral research fellow, Medical School, Birmingham University, Birmingham, UK; Degrees: Ph.D., Protein Chemistry, Leeds University, Leeds, UK; M.Sc. Fiber Science, Leeds University, Leeds, UK.